Article:
Yang, Z, Zhai, X, Zou, X et al. (7 more authors) (2021) Bilayer pH-sensitive colorimetric films with light-blocking ability and electrochemical writing property: Application in monitoring crucian spoilage in smart packaging. Food Chemistry, 336. 127634. ISSN 0308-8146

https://doi.org/10.1016/j.foodchem.2020.127634

Bilayer pH-sensitive colorimetric films with light-blocking ability and electrochemical writing property: application in monitoring crucian spoilage in smart packaging

Zhikun Yang [a], Xiaodong Zhai [a], Xiaobo Zou [a,*], Jiyong Shi [a,*], Xiaowei Huang [a], Zhihua Li [a], Yunyun Gong [b], Melvin Holmes [b], Megan Povey [b], Jianbo Xiao [c]

[a] Agricultural Product Processing and Storage Lab, School of Food and Biological Engineering, Jiangsu University, Zhenjiang, Jiangsu 212013, China

[b] School of Food Science and Nutrition, University of Leeds, Leeds LS2 9JT, United Kingdom

[c] Institute of Chinese Medical Sciences, State Key Laboratory of Quality Research in Chinese Medicine, University of Macau, Taipa, Macau, China

[*]Corresponding author. Tel.: +86 511 88780174; Fax: +86 511 88780201; Email: zou_xiaobo@ujs.edu.cn (Xiaobo Zou), Shi_jiyong@ujs.edu.cn (Jiyong Shi).

Abstract

Bilayer colorimetric films were developed for monitoring fish spoilage by using gelatin (GN) incorporated with ZnO nanoparticles as the upper layer (GN-ZnO), and gellan gum (GG) incorporated with mulberry anthocyanins (MBA) as the lower layer (GG-MBA). The color stability of the bilayer colorimetric films under visible and ultraviolet light was improved with the increase of ZnO nanoparticles content. Meanwhile, the bilayer films had good NH_3 sensitivity. The limit of detection of the GG-MBA/GN-2.0% ZnO film to NH_3 was 0.01 mM. The electrochemical writing ability of the bilayer films was also identified, indicating the feasibility of inks-free printing on biopolymer films. Finally, the GG-MBA/GN-2.0% ZnO film with an electrochemical writing pattern was used to monitor crucian spoilage. The GG-MBA/GN-2.0% ZnO film with electrochemical writing pattern showed visible color changes with the crucian spoilage. In conclusion, the bilayer colorimetric film was expected to be a good fish spoilage indicator in smart packaging.

Keywords: Bilayer colorimetric film; Gelatin; Gellan gum; ZnO nanoparticles; Mulberry anthocyanins; Electrochemical writing

Introduction

Safety and quality control of foods have attracted significant global attentions (Valdez, Gupta, Lozano, & Mao, 2019). It is well-known that fish is popular with consumers owing to high protein content and nutritional qualities. However, it is perishable due to enzymatic reactions and microbial contamination (X. Zhang, Sun, Xiao, Liu, & Zheng, 2016). Volatile amines, such as trimethylamine, dimethylamine, and ammonia (NH_3), are the degradation products of amine acids and proteins due to microbial growth, and generally known as total volatile basic nitrogen (TVB-N). TVB-N levels have been widely used as the indicator of fish spoilage (Zhai, Shi, Zou, Wang, Jiang, Zhang, et al., 2017).Therefore, the sensitive detection of TVB-N is critical for evaluating the quality and safety of fish products (Erim, 2013). In addition, to provide essential manufacturing information to consumers, most food packaging materials are labeled with inks that mainly consist of petrochemical feedstock, which can potentially contaminate the food and environment, and even endanger human health (Patel, 2015; Wu, Wang, Yan, Ding, Shi, Deng, et al., 2018). Thus, there is a great demand for developing edible labels to minimize food safety risk.

Recently, many studies have concentrated on developing smart packaging for tracing food quality. In particular, pH-sensitive colorimetric films have been widely explored, because they can present color changes when exposed to volatile gases, such as biogenic amines generated from foods (Huang, Xiong, Zou, Dong, Ding, Liu, et al., 2019). Generally, a pH-sensitive colorimetric film is composed of solid supports and dyes (Pourjavaher, Almasi, Meshkini, Pirsa, & Parandi, 2017). In recent years, anthocyanins, as edible natural pigments, have been used to develop colorimetric films due to their non-toxic and pH-sensitive properties (Choi, Lee, Lacroix, & Han, 2017; Huang, et al., 2019; Jr, Arruda, & Stefani, 2015; Zhai, et al., 2017). To immobilize the anthocyanins, various polymeric compounds have been utilized as solid supports (Choi, Lee, Lacroix, & Han, 2017; Huang, et al., 2019; Wei, Cheng, Ho, Tsai, & Mi, 2017; Zhai, Li, Zhang, Shi, Zou, Huang, et al., 2018). The color stability of anthocyanins to ultraviolet (UV) light, temperature, and oxygen are important for the colorimetric films in practical application (Bąkowska, Kucharska, & Oszmiański, 2003; Xuran Cai, Du, Cui, Wang, Yang, & Zhu, 2019). Particularly, UV light showed a significant influence on the stability of anthocyanins over other factors (Bąkowska, Kucharska, & Oszmiański, 2003; Tonon, Brabet, & Hubinger, 2010). Therefore, it is essential to improve the stability of anthocyanins embedded in colorimetric films.

Nano metal oxides have attracted much attention in the field of smart packaging materials due to their excellent biocompatibility and functional property (Xuechao Cai, Xie, Li, Kassymova, Zang, & Jiang, 2020; Chandra, Kumari, Bontempi, & Yadav, 2020; Varma, 2012). Zinc oxide (ZnO) is an inorganic compound and is currently listed as a generally safe (GRAS) material by the Food and Drug Administration (21CFR182.8991). It has efficient UV absorptivity resulting from its wide bandgap (Eg = 3.37 eV, corresponding to 376 nm UV light). Moreover, gelatin (GN) has been widely used as a film-forming agent because of its out-standing gel formability (Hosseini & Gómez-Guillén, 2018; Quero, Padilla, Campos, Luengo, Caballero, Melo, et al., 2018). Our previous work revealed that multicolor patterns could be marked on the protein/polysaccharide/anthocyanin composite films by electrochemical writing (Zhai, et al., 2018). The electrochemical writing process based on the pH-responsive color change of anthocyanins provides a green printing method for presenting the essential information of the product, such as the storage information and nutritional facts of the food in a safe fashion. However, to the best of our knowledge, there are few studies on printing on biopolymer films (Wu, et al., 2018; Zhai, Li, Shi, Huang, Sun, Zhang, et al., 2019).

The aims of this study were: (1) to design a bilayer colorimetric hydrogel film with UV light

blocking capability and electrochemical writing properties and (2) to monitor the spoilage of crucian fish in real-time. ZnO nanoparticles were incorporated in gelatin (GN) as the upper layer to improve the light-blocking property of the film. The lower layer of the film consisted of gellan gum (GG) and anthocyanin extracted from mulberry fruits (MBA), which is a traditional anthocyanin-rich fruit (Zeng, Chen, Qin, Zhang, Wang, Wang, et al., 2019). GG is a natural extracellular polysaccharide produced by fermentation of *Sphingomonas paucimobilis*, which has been widely used as an edible food additive and in polymer films (Amin & Panhuis, 2011; Wei, Cheng, Ho, Tsai, & Mi, 2017). The GG-MBA composite with NH_3 sensitivity was used as the lower layer to indicate fish freshness.

2. Material and methods

2.1. Materials and Reagents

Mulberry fruits (*Morus nigra L*), and Crucian (*Carassius carassius*) were obtained from a local supermarket (Zhenjiang, China). Other chemical agents, such as low-acyl gellan gum, gelatin, ZnO nanoparticles, ammonium hydroxide, and ethyl alcohol were purchased from Sinopharm Chemical Reagent Co., Ltd. (Shanghai, China).

2.2. Anthocyanins extraction and its response to pH variation

The anthocyanins in mulberry fruits were extracted according to our previous method (Yang, Zou, Li, Huang, Zhai, Zhang, et al., 2019). Firstly, the dried mulberry fruits were ground with an electric coffee mill. The powder was prepared in 60% ethanol aqueous solution with a solid-liquid ratio of 1:50 and stirred for 30 min by using a magnetic stirrer. Then the extract solution was filtered through a 25-μm filter paper, concentrated using a vacuum rotary evaporator and freeze-dried to obtain the extract powder. The obtained MBA extract powder was stored at 4 °C in brown air-tight plastic bottle. The spectra at 400-800 nm of MBA solutions under pH 2-12 were determined by using the UV-Vis spectrophotometer (GNilent CARY 100, Varian Corporation, USA). The pH of MBA solutions was adjusted by using 0.2 M disodium hydrogen phosphate, 0.2 M citric acid and 0.2 M sodium hydroxide solutions with different proportions.

2.3. Development of bilayer films

The solution of GN was prepared by dissolving 2 g of GN powder in 100 mL distilled water while heating at 80 °C in a water bath under magnetic stirring for 1 h. Thereafter, different amounts of ZnO nanoparticles were added to the GN solution at 0.5 mg ZnO/g GN, 1 mg ZnO/g GN and 2 mg ZnO/g GN, expressed as GN-0.5% ZnO, GN-1.0% ZnO, and GN-2.0% ZnO. Subsequently, the mixture was homogenized (Ultra Turrax IKA T25 digital, Germany) at 8000 rpm for 5 minutes and degassed for 5 minutes at 80 °C using a sonicator (Branson CPX 5800H, USA). After degassing, 6 g of the GN-ZnO solution was instantly poured into a plastic Petri dish as the upper layer of the bilayer hydrogel. The solutions formed hydrogels after cooling.

The solution of GG was prepared by dissolving 2 g of GG powder in 100 mL distilled water at 95 °C under magnetic stirring for 1 h. 4 mg of MBA powder was then added to the GG solution (65 °C). Under this constant temperature, 40 mg of $CaCl_2{\cdot}2H_2O$ was completely dissolved into the solution with constant stirring. The GG-MBA mixture was degassed with a sonicator, and then 6 g of GG-MBA solution was instantly poured over the GN-ZnO layer hydrogel. The GG-MBA solution formed to be the lower layer of the bilayer hydrogel after cooling.

Meanwhile, the bilayer hydrogels containing GG, GN, and $CaCl_2{\cdot}2H_2O$, or containing GG, GN, $CaCl_2{\cdot}2H_2O$, and MBA were also prepared, following the same process. The bilayer hydrogels containing MBA were selected for electrochemical writing. The cooled bilayer hydrogels were placed on a platinum (Pt) plate connected with the cathode of an electrochemical analyzer (CHI660E, CH Instruments Co.,

Shanghai, China). Then, a 0.5-mm Pt needle connected to the anode of the electrochemical analyzer was contacted the surface of the GG-MBA hydrogel. The electrochemical writing process was performed according to our previous method (Zhai, et al., 2018). All bilayer hydrogels were heated in an oven at 40 °C for 4 h to form films, and the films were placed at 4 °C with 75% relative humidity (RH) before use.

2.4. Characterization of the films

The cross-section of the films was observed under a field emission scanning electron microscopy (FE-SEM) (S-4800, Hitachi High Technologies Corporation, Japan) coupled with energy dispersive X-ray (EDX). The films were freeze fractured by liquid nitrogen for cross-section observation. Then, they were attached to double-sided conductive adhesive tape and mounted on the specimen holder. Finally, the films were coated with gold under vacuum. The optical transmittance of the films was measured at 200-800 nm using the UV–Vis spectrophotometer.

2.5. Color stability

To simulate the indoor and outdoor light conditions, the films were stored in the incubator at 25 °C with 75% RH under fluorescent lights (~ 400-760 nm) and UV light (λ = 365 nm, 100 W, Spectroline SB-100P, Sylvania, USA), respectively. The photos of the films were captured using an optical scanner (Scanjet G4050, HP) and analyzed using a user program in Matlab R2012a (Matworks Inc., Natick, MA, USA). The stability of the films was defined as the relative color change (S), according to our previous study (Xiao-wei, Xiao-bo, Ji-yong, Zhi-hua, & Jie-wen, 2018).

$$\Delta R=|R_0-R_1| \quad (1)$$

$$\Delta G=|G_0-G_1| \quad (2)$$

$$\Delta B=|B_0-B_1| \quad (3)$$

$$S(\%)=\frac{\Delta_R+\Delta_G+\Delta_B}{R_0+G_0+B_0}\times 100 \quad (4)$$

where R_0, G_0, B_0 were the initial gray values of the red, green and blue, R_1, G_1, and B_1 were the gray values of the red, green and blue after storage. S was the relative color change of R, G and B values.

2.6. NH_3-sensing ability

The NH_3 was used to determine the color response of the film towards basic gas. Briefly, the films (10×10 mm) were placed in an Erlenmeyer flask (500 mL) containing different concentrations of ammonia solution for 30 min at 25 °C. The images of the films were captured using the optical scanner, and the S value of the films was measured as described in Section 2.5. The spectra of the films at 400-800 nm were documented by means of the UV–Vis spectrophotometer.

2.7. Application of films in monitoring fish spoilage

For the fish spoilage test, 200 g of crucian, after removing its tail, innards and scales, was put into a polyethersulfone resin (PES) box with a lid. The hole (15 × 15 mm) on the lid was covered by using a piece of GG-MBA/GN-ZnO film (20 × 20 mm) with a written pattern. The PES box was placed in an incubator at 4 °C with 75% RH. The TVB-N content of the crucian was measured according to our previous method (Zhai, et al., 2018), following the Chinese standard (GB 5009.228-2016).

2.8. Statistical analysis

Duncan's multiple range test was used to compare the means at the 95% confidence level by using SPSS statistics software. The data labeled with different lowercase letters are significantly different.

3. Results and discussion

3.1. Color and spectral properties of MBA

Fig. 1a shows the color changes of MBA solution under different pH conditions. The MBA solution

presented a remarkable color change from light pink to colorless at pH 2-6. When the pH increased from 7 to 10, the color of the MBA solution changed gradually from light green to yellow-green and presented an orange color at pH 11-12. The corresponding UV-Vis spectra of the MBA solution in different pH buffer solutions are shown in Fig. 1b. When the pH increased from 2 to 6, the maximum absorption peak (MAP) of the MBA solution at 526 nm gradually decreased, and then underwent a shift from 526 nm to 592 nm when the pH increased from 6 to 7. The MAP at 592 nm gradually increased when the pH increased from 7 to 10, and then decreased sharply at pH 10-12. The intensity of green compared to red color could be expressed by the absorbance ratio at 592 nm versus 526 nm (A_{592}/A_{526}).The inset in Fig.1b shows an exponential relationship between A_{592}/A_{526} and pH 2-9. Expressing the following formula:

$$y=0.3479e^{0.12x} \quad (5)$$

where x is the pH and y is the absorbance ratio at 592 nm versus 526 nm:

The value of A_{592}/A_{526} increased when the pH increased from 2 to 9, indicating a deeper green color. The values decreased with the pH increased from 10 to 12. Similarly, Zhai, et al. (2018) also reported that the absorbance ratio of red radish anthocyanins had good exponential relationships with the pH values among 2 to 9, and then the values decreased with the pH increase from 10 to 12. These results indicated that MBA could be used as the natural pH-sensitive pigments for colorimetric films.

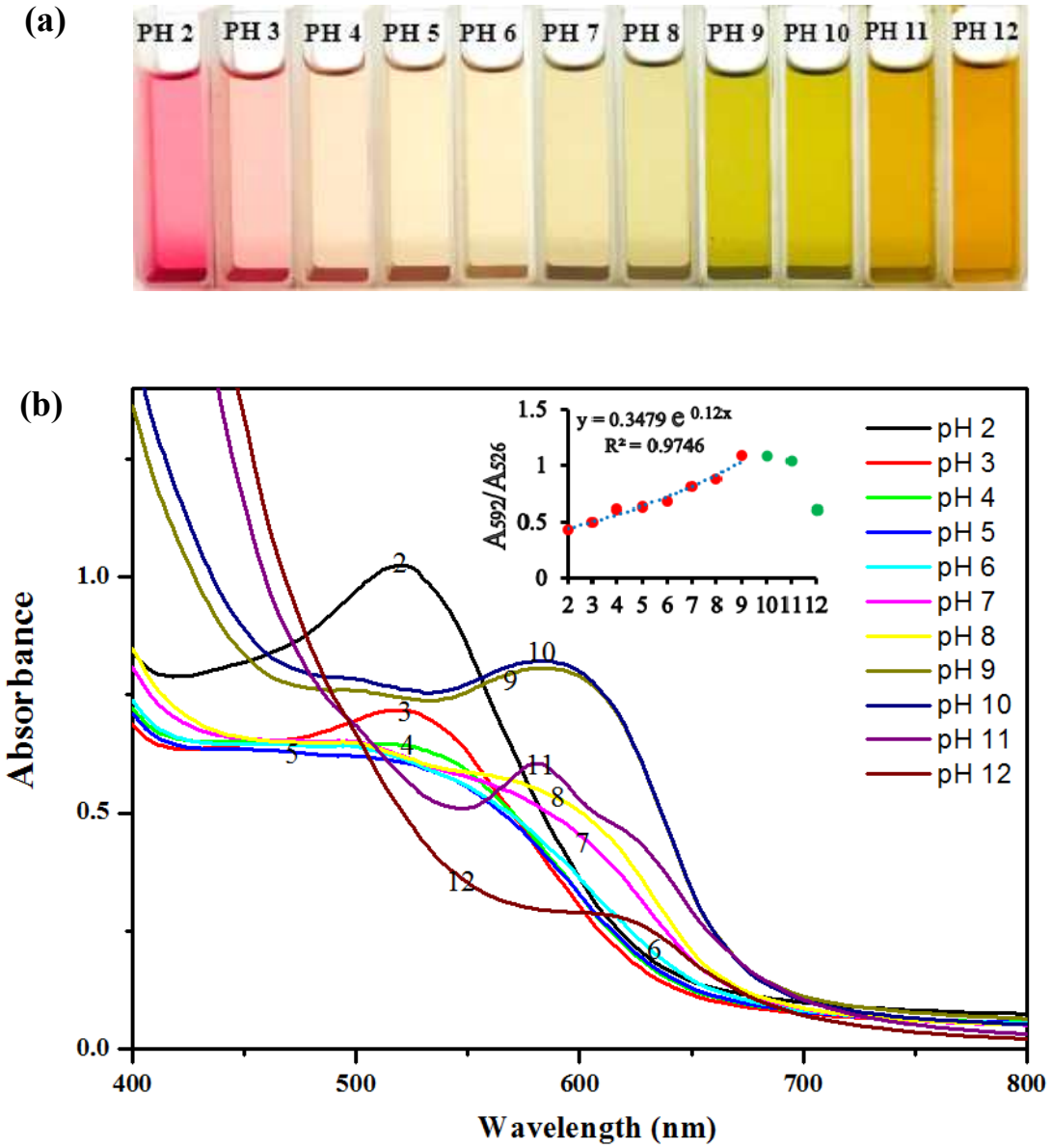

Figure. 1. Color changes (a) and UV-Vis spectra of MBA solutions at different pH (b).

3.2. Morphological and EDX analysis

The cross-section of the GG layer was comparatively smooth and homogeneous, while the GN layer was less homogeneous with some cracks (Fig. 2a). A bilayer structure could be clearly seen from the GG/GN film. This could be due to GG molecules and calcium ions form a stable gel structure, making GG immiscible with GN during the thermal drying process. The GG and GN layer represented a continuous matrix with good structural integrity, and there was no obvious gap between the two layers. This could be due to that GN and GG can be partially cross-linked through hydrogen bonding force. Fig. 2b shows that the cross-section of the GG layer altered little with the addition of the MBA. The sheet polyhedral shapes ZnO nanoparticles were agglomerated to clusters as observed in the FE-SEM (Fig. 2c). Fig. 2d shows that little granular protrusion was observed in the cross-section of GG-MBA/GN-0.5% ZnO, indicating that the ZnO nanoparticles were well distributed and have good miscibility with the GN. With the increase of ZnO content, the GN-ZnO layer indicated some irregularities representative of semi-crystalline structures (Fig. 2e and 2f), which are related to the presence of the degree of crystallinity of ZnO nanoparticles. All the GG-MBA/GN-ZnO films showed that the interface of the GG-MBA layer

and GN-ZnO layer maintained well-crosslinked, and the ZnO nanoparticles in GN-ZnO layer did not move to the GG-MBA layer. The EDX analysis was also performed to identify the element composition of the bilayer film (Fig. S1). The signal related to Zn and O was found in the spectrum, which confirmed the presence of ZnO in the bilayer film. These results revealed that we developed the GG-MBA/GN-ZnO bilayer films with satisfactory distribution and integrity.

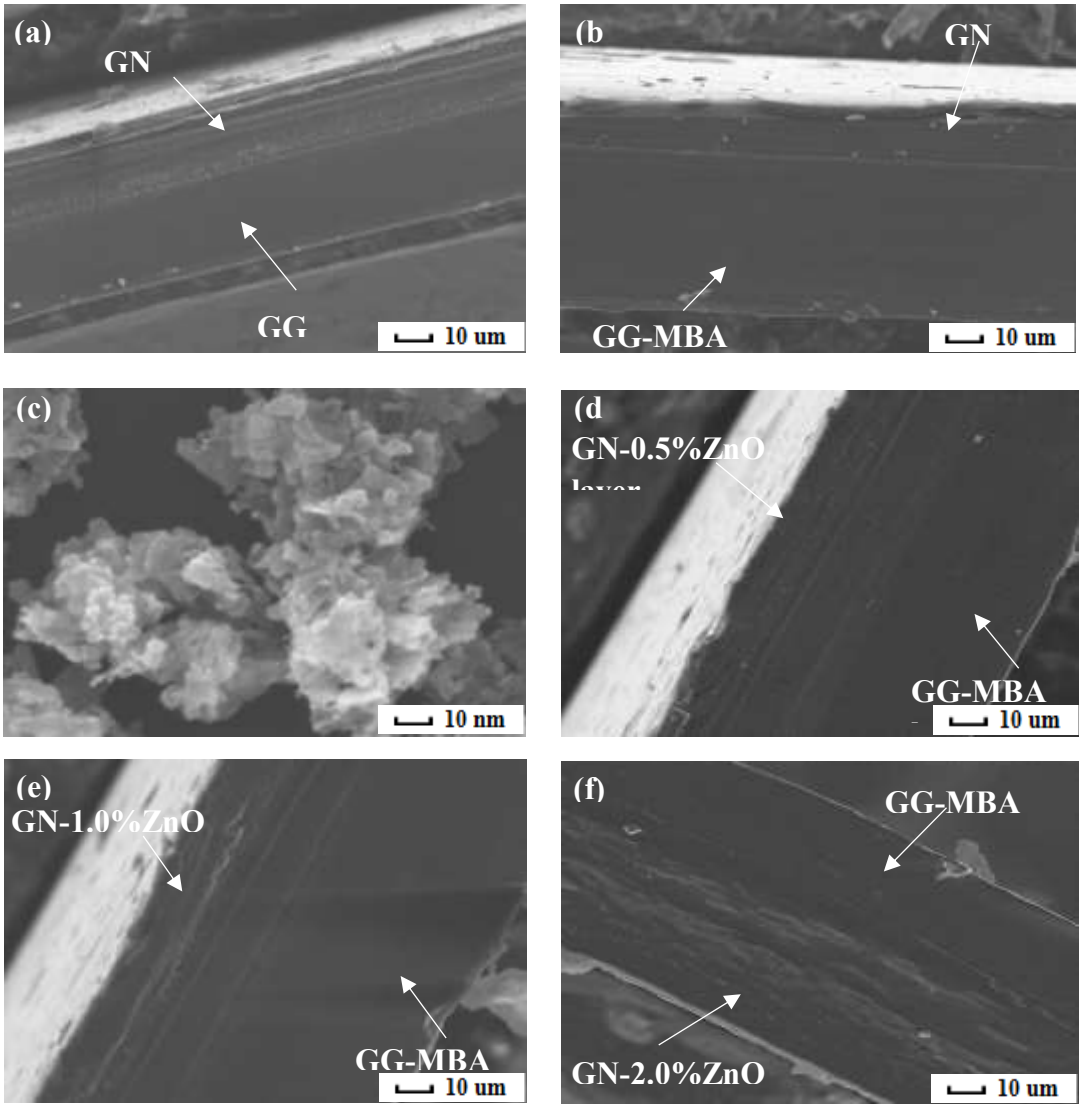

Figure. 2. SEM images of cross section of GG/GN (a), GG-MBA/GN (b), ZnO nanoparticles (c), GG-MBA/GN-0.5% ZnO (d), GG-MBA/GN-1.0% ZnO (e) and GG-MBA/GN-2.0% ZnO film (f).

3.3. Optical property and color stability of the bilayer films

The UV/vis transmission spectra of the bilayer films are shown in Fig. S2. The transmission of the GG/GN film was > 61.6% at 400-800 nm, and decreased slightly with the incorporation of the MBA. The visible light transmittance (400-650 nm) of colorimetric film furtherly decreased with the incorporation of ZnO. The decrease in the visible light transmission of the ZnO-incorporated colorimetric film was mainly attributed to the ZnO nanoparticles in the bilayer film that could hinder the passage of light (Kanmani & Rhim, 2014; X. Liu, Chen, Ren, Chang, He, & Zhang, 2019; Wang, Gong, Miao, Guo, Liu, Fan, et al., 2019). It is interesting to note that the ZnO-incorporated colorimetric film presented excellent UV-blocking property, and this property of the film further improved with the increasing concentration of ZnO. The blocking of the UV spectrum was due to the ZnO in the upper layer film with

band-gap energy of 3.2 eV, that can absorb a larger fraction of UV light (Lupan, Postica, Pauporté, Hoppe, & Adelung, 2019; Shankar, Teng, Li, & Rhim, 2015; Wang, et al., 2019). Such UV-blocking properties have also been observed with other biopolymer films (Lizundia, Ruiz‐Rubio, Vilas, & León, 2016; Oun & Rhim, 2017; Shankar & Rhim, 2017).

The color stability of the anthocyanins embed in the colorimetric film is essential for practical application. Fig. 3a shows the color change of the films exposed to visible light at 25 °C for 24 d. During the storage, the color of the GG/GN film was well-preserved. All colorimetric films were faded to yellow after exposure to visible light for 24 days. The S value of the film was determined as the measure of the degree of discoloration. As can be seen in Fig. 3b, the S value of the GG/GN film exposed to visible light remained almost constant (< 1%). This indicated that GG/GN as a composite material was light-stable. As for bilayer colorimetric films, the S value increased slightly during the storage period. At the end of the storage, the S value of GG-MBA/GN film was increased to 5.61%. However, the S value of the GG-MBA/GN-0.5% ZnO film was only 3.41%, and when the content of ZnO increased to 2.0%, the S value of the bilayer films further decreased to 1.75%. This was in agreement with the fact of the light-blocking property (Fig. S2) and oxygen barrier property (Table S1) of ZnO that protected the anthocyanins from degradation. Fig. 3c shows the color change of the films exposed to UV light at 25 °C for 32 h. The GG/GN film exhibited a stable gray color during the storage period. After 32 h of storage, the color of bilayer colorimetric films faded to yellow. Meanwhile, all colorimetric films presented high S values under the UV light (Fig. 3d), indicating that the stability of mulberry fruit's anthocyanins was significantly affected by UV light (Aramwit, Bang, & Srichana, 2010). During the storage period, the S value of the GG-MBA/GN-ZnO films was lower than the GG-MBA/GN film, and decreased with the increasing concentration of ZnO. This was due to the UV-light absorption function of the ZnO nanoparticles (Fig. S2) (Kubacka, Fernandez-Garcia, & Colon, 2011). The UV light absorbing ability could decrease the degradation of MBA in the lower layer film. The above-mentioned results indicated that ZnO nanoparticles could be used as a UV blocking agent to enhance the color stability of the film.

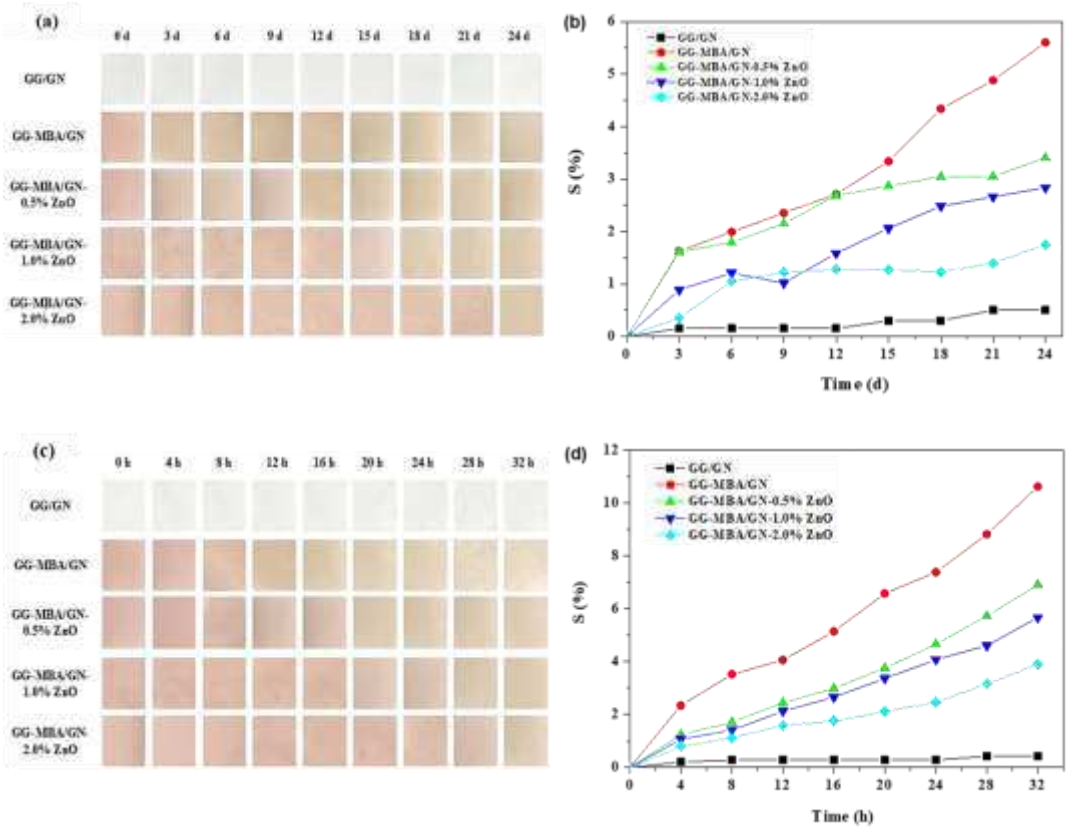

Figure. 3. Transparency spectrum of the bilayer films (a); the color changes (b) and S value (c) of the bilayer films under visible light, and the color changes (d) and S value (e) of the bilayer films under UV light.

3.4. Electrochemical writing on bilayer film

A bilayer hydrogel with excellent structural stability was firstly produced in this work. The picture of the triangle pattern written on the GG-MBA/GN-2.0% ZnO film under different positive currents (the positive current direction is from Pt needle to Pt plate) and negative current (the negative current direction is from Pt plate to Pt needle) are shown in the Fig. 4a. The triangle pattern was light pink when the current was 1 mA, and turned to pink with the current increase to 8 mA. This accord with the fact that the surface of the GG-MBA hydrogel will generate hydrogen ions due to the anodic water electrolysis reaction while it connected with the Pt needle. Thus, the structure of MBA in the GG hydrogel transformed from anhydrobase to flavylium ion, and the MBA changed to light pink. With the increase of the current, the water electrolysis reaction on the surface of the hydrogel became more intense; thus, generating more hydrogen ions so that more anhydrobase transformed to flavylium ion. Finally, the color of MBA embeds in the film changed to pink. With the current increased from −1 mA to −8 mA, the triangle pattern gradually changed from light green to yellow-green and finally a yellow color. This accord with the fact that the surface of the GG-MBA hydrogel will generate hydroxide ions due to the cathodic water electrolysis reaction while it connected with the Pt needle. Hence, the structure of MBA in the GG hydrogel transformed from anhydrobase to anhydrobase anion, and the MBA changed to light green. With the increase of the current, the cathodic water electrolysis reaction on the surface of the hydrogel became more intense; thus, generating more hydroxide ions so that more anhydrobase transformed to anhydrobase anion. Finally, the color of MBA embeds in the film changed to yellow. As shown in Fig. 4b, 4c, and 4d, the two-color hourglass, multicolor flower, and the Chinese characters were successfully

written on the bilayer colorimetric films. This electrochemical writing process is reliable and programmable. Meanwhile, the electrochemical writing on the film will also broaden the application of the film.

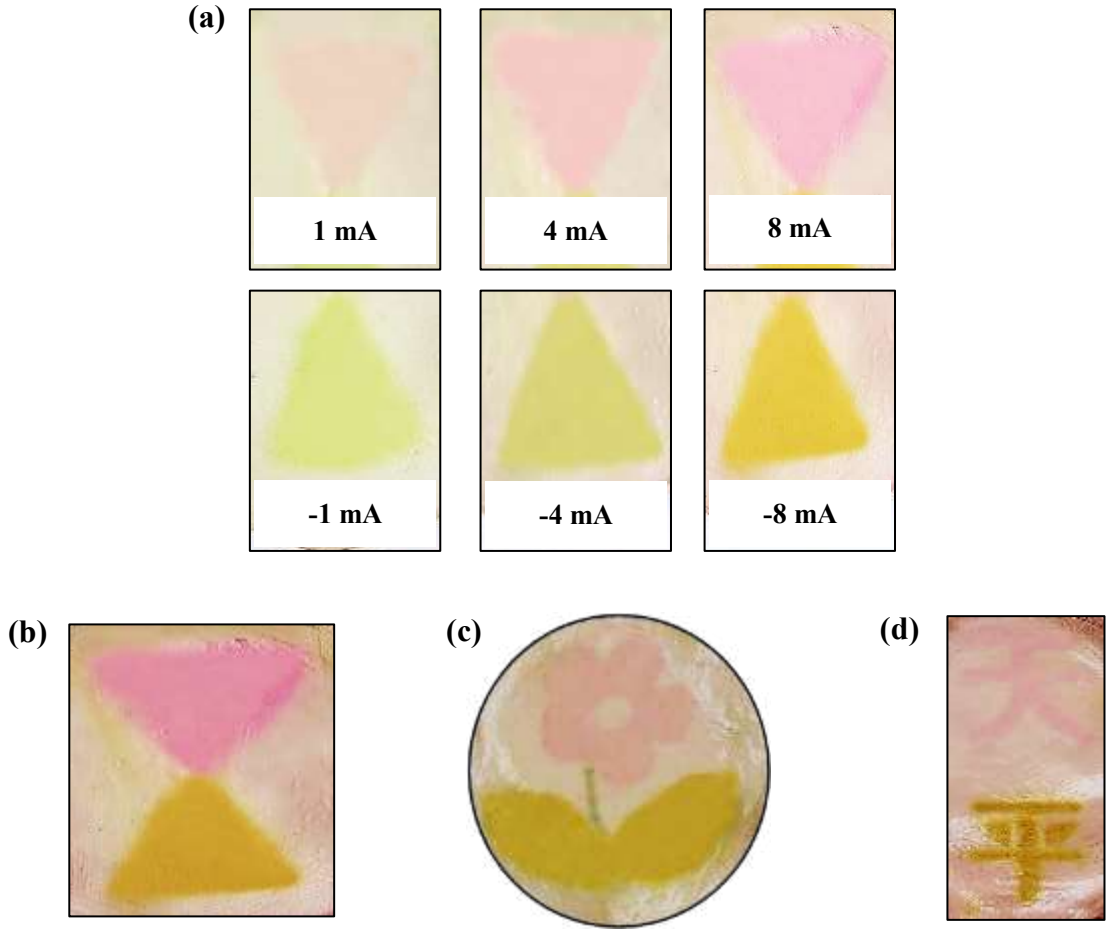

Figure. 4. The images of triangle pattern written on the GG-MBA/GN-2.0% ZnO film under different currents (a); the images of hourglass (b), flower (c), and the Chinese characters (d) written on the GG-MBA/GN-2.0% ZnO film.

3.5. NH_3 sensing analysis

The gas-sensing ability of the colorimetric film is essential for practical application in monitoring the freshness (J. Zhang, Zou, Zhai, Huang, Jiang, & Holmes, 2019). Hence, the response of the bilayer colorimetric film to NH_3 was tested in this work. The color changes (inset) and the corresponding S value of the bilayer colorimetric films toward different concentrations of NH_3 are shown in Fig 5a. With the increasing concentration of NH_3 (0-0.10 mM), all the films gradually turned from pink to green and finally a yellow color. This was due to the fact that volatile NH_3 could combine with H_2O embedded in the colorimetric film and hydrolyze into OH^- ions and produced an alkaline environment. Finally, the color of the film was changed due to the structure of anthocyanins transformed from flavylium ion to anhydrobase anion in the presence of hydroxyl ions (J. Liu, Wang, Guo, Li, Chen, Jiang, et al., 2019). When the bilayer colorimetric films reacted with different concentrations of NH_3, no obvious difference was observed in terms of their color change, corresponding S value, and corresponding UV-Vis spectra (Fig. 5b, S3, S4 and S5). The aforementioned results indicated that the incorporation of ZnO nanoparticles had no negative effect on the NH_3-sensing ability of colorimetric film. Moreover, the UV-Vis spectra of the GG-MBA/GN-2.0% ZnO film when reacted with different concentrations of NH_3 is

shown in Fig. 5b. With the increasing concentration of NH_3, the absorption peak at 497 nm decreased from 0.44 to 0.37, and the absorption peak at 614 nm gradually increased from 0.29 to 0.32. This indicated that the GG-MBA/GN-2.0% ZnO film gradually transferred to be more basic. The intensity of green color compared to red color was represented by the absorbance ratio at 614 nm versus 497 nm (A_{614}/A_{497}). As can be seen in the inset of Fig. 5b, the A_{614}/A_{497} shows a linear relationship with NH_3 concentration (0-0.08 mM). Expressed the following formula:

$$y=3.0x+66,\ R^2=0.99 \quad (6)$$

where x is the NH_3 concentration and y is the absorbance ratio at 614nm versus 497 nm:

The absorbance ratio at 614nm versus 497 nm of GG-MBA/GN-2.0% ZnO film gradually increased with the increase of NH_3 concentration (0-0.08 mM), while it decreased when NH_3 concentration was up to 0.10 mM. Meanwhile, the limit of detection (LOD) of GG-MBA/GN-2.0% film toward NH_3 was also determined by the following formula:

$$LOD=\frac{3K}{N} \quad (7)$$

Where K is the standard deviation of blank measurements (n = 15) and N is the slope of the calibration curve.

The LOD of GG-MBA/GN-2.0% ZnO film to NH_3 was 0.01 mM, indicating the GG-MBA/GN-2.0% ZnO film could be used as a gas sensor to monitor the NH_3.

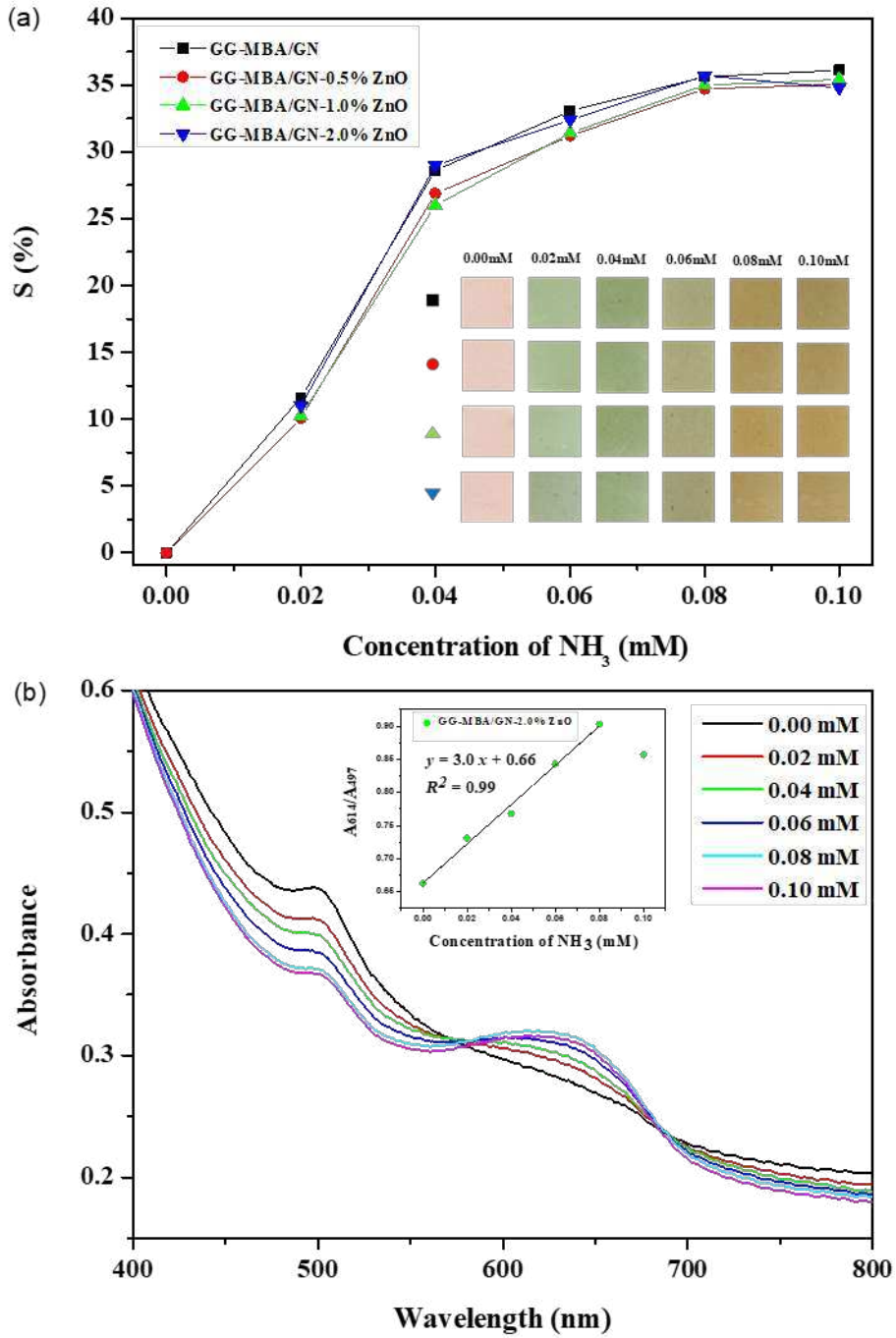

Figure. 5. The S value (a) and color changes (inset) of the bilayer colorimetric films after exposure to different concentrations of NH_3, and the UV-Vis spectra of GG-MBA/GN-2.0% ZnO film after exposure to different concentrations of NH_3 (b).

3.6. Application of film for indicating fish spoilage

In our initial trial, the tensile strength (TS), elongation at break (EB), water vapor permeability (WVP) and oxygen permeability (OP) of the bilayer films were measured (Table S1). Although the GG-MBA/GN-1.0% ZnO presented a quite higher TS, the GG-MBA/GN-2.0% ZnO film presented the optimal performance on EB, UV-blocking property, color stability, and NH_3-sensing ability. Hence, the

GG-MBA/GN-2.0% ZnO film was selected to monitor the crucian spoilage. The rectangular pattern was printed on GG-MBA/GN-2.0% ZnO film by means of electrochemical writing. As shown in Fig. 6a, 6b, and 6c, the color change of the film, corresponding color parameters (R, G, and B) and corresponding TVB-N content were changed with the change of the crucian freshness at 4 °C. The initial TVB-N value of the fresh crucian was 4.7 mg/100g and the color of the film was pink. After ~6 days of storage, the TVB-N value was increased to 20.7 mg/100g. Meanwhile, the color of the film was changed to light green, and the corresponding R, G and B values were recorded as ~190, ~192 and ~128, respectively. The limit of TVB-N content of fish in Chinese standard specification GB/T 5009.228 (2016) is 20 mg/100 g, indicated that the crucian was inedible at this stage. The TVB-N value reached 40.7 mg/100g at 9 d and the film reached a final yellow-green color, and the corresponding R and B value of the GG-MBA/GN-2.0% ZnO film decreased to 185 and 118, which was consistent with the color change of the film. It is interesting to note that the rectangular pattern formed by electrochemical writing was maintained clearly during the storage period, indicating the stability of electrochemical writing information. These results showed that the GG-MBA/GN-2.0% ZnO film with written patterns was expected to be a biological sensor for detecting the spoilage of crucian.

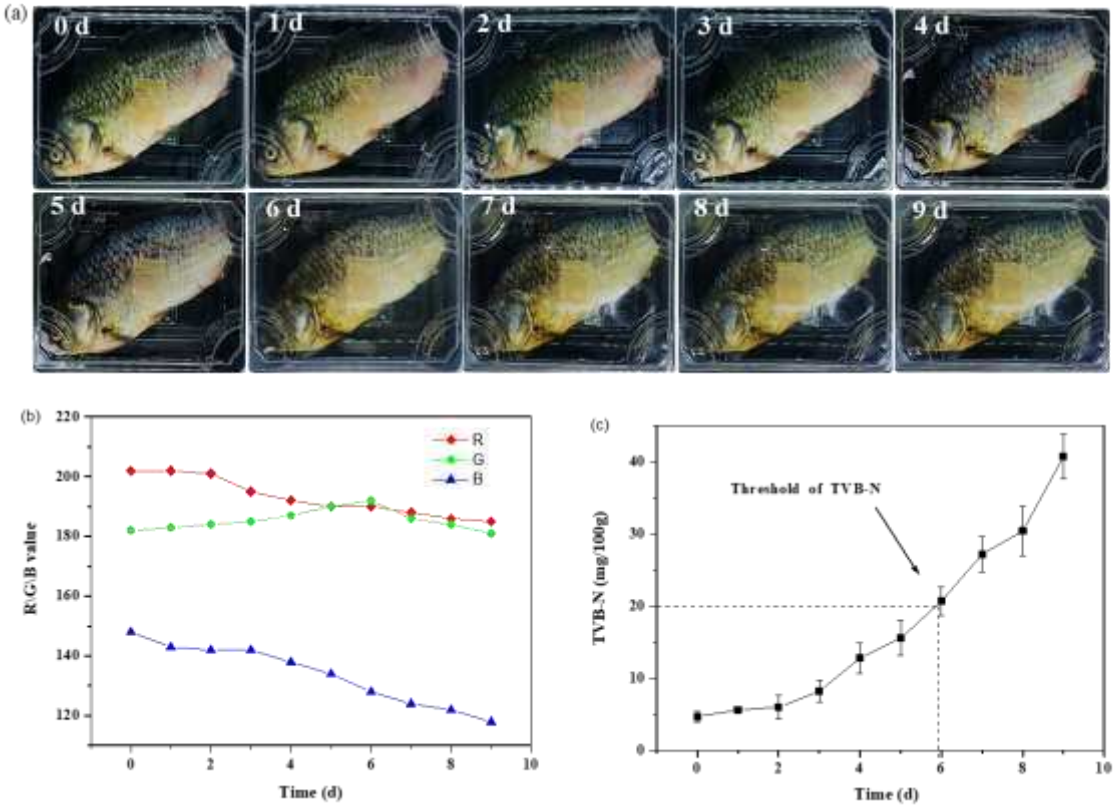

Figure. 6. Images of GG-MBA/GN-2.0% ZnO film with a written pattern for monitoring the spoilage of crucian (a), corresponding R, G, and B value changes of the film (b), and the TVB-N level of the crucian (c).

3.7. Safety and cost of the film

The bilayer colorimetric film is cost-effective and presented low toxicity. GG is a natural extracellular polysaccharide, which has currently listed as an edible additive in many food products by both U.S. FDA and the EU (E418). GN as a biopolymer derived from collagen has been widely used in the food industry (Farshchi, Pirsa, Roufegarinejad, Alizadeh, & Rezazad, 2019). In addition, ZnO nanoparticle is an

inorganic compound, which has received U.S. FDA approval for application as a generally safe (GRAS) material and has previously used as an antimicrobial additive (Espitia, Soares, Teófilo, Coimbra, Vitor, Batista, et al., 2013). The cost of the chemicals involved for one thousand bilayer hydrogels is merely $19.21 (Table S2). Hence, the bilayer colorimetric film is a safe and economical sensor for smart food packaging.

4. Conclusions

Bilayer colorimetric films with electrochemical writing ability were developed for monitoring the fish freshness. SEM images indicated that the bilayer film was fabricated successfully. The addition of ZnO nanoparticles significantly improved the illumination stability of the bilayer film, while did not produce interference on the NH_3-sensing ability of the films. The LOD of GG-MBA/GN-2.0% ZnO film to NH_3 was 0.01 mM. The bilayer colorimetric films performed visible color changes with the crucian spoilage, and the patterns written on the films were well-maintained. Thus, the developed colorimetric film with written patterns was expected to be a safe, low-cost and non-destructive indicator for monitoring the fish spoilage during storage.

Acknowledgments

This work was supported by the National Natural Science Foundation of China (31671844, 31601543, 31801631, 31772073), the National Key Research and Development Program of China (2016YFD0401104, 2017YFC1600805, 2018YFD0400803, 2017YFC1600806, 2017YFD0400102-3, 2018YFD0701001) and the Natural Science Foundation of Jiangsu Province (BK20160506, BE2016306, BK20180865).

Supplementary data

Some essential tables and figures were added.

Reference

Amin, K. A. M., & Panhuis, M. I. H. (2011). Polyelectrolyte complex materials from chitosan and gellan gum. *Carbohydrate Polymers, 86*(1), 352-358.

Aramwit, P., Bang, N., & Srichana, T. (2010). The properties and stability of anthocyanins in mulberry fruits. *Food Research International, 43*(4), 1093-1097.

Bąkowska, A., Kucharska, A. Z., & Oszmiański, J. (2003). The effects of heating, UV irradiation, and storage on stability of the anthocyanin – polyphenol copigment complex. *Food Chemistry, 81*(3), 349-355.

Cai, X., Du, X., Cui, D., Wang, X., Yang, Z., & Zhu, G. (2019). Improvement of stability of blueberry anthocyanins by carboxymethyl starch/xanthan gum combinations microencapsulation. *Food Hydrocolloids, 91*, 238-245.

Cai, X., Xie, Z., Li, D., Kassymova, M., Zang, S.-Q., & Jiang, H.-L. (2020). Nano-sized metal-organic frameworks: Synthesis and applications. *Coordination Chemistry Reviews, 417*, 213366.

Chandra, H., Kumari, P., Bontempi, E., & Yadav, S. (2020). Medicinal plants: Treasure trove for green synthesis of metallic nanoparticles and their biomedical applications. *Biocatalysis and Agricultural Biotechnology, 24*, 101518.

Choi, I., Lee, J. Y., Lacroix, M., & Han, J. (2017). Intelligent pH indicator film composed of agar/potato starch and anthocyanin extracts from purple sweet potato. *Food Chemistry, 218*, 122-128.

Erim, F. B. (2013). Recent analytical approaches to the analysis of biogenic amines in food samples. *Trac Trends in Analytical Chemistry, 52*(52), 239-247.

Espitia, P. J. P., Soares, N. d. F. F., Teófilo, R. F., Coimbra, J. S. d. R., Vitor, D. M., Batista, R. A., Ferreira, S. O., de Andrade, N. J., & Medeiros, E. A. A. (2013). Physical–mechanical and antimicrobial properties of nanocomposite films with pediocin and ZnO nanoparticles. *Carbohydrate Polymers, 94*(1), 199-208.

Farshchi, E., Pirsa, S., Roufegarinejad, L., Alizadeh, M., & Rezazad, M. (2019). Photocatalytic/biodegradable film based on carboxymethyl cellulose, modified by gelatin and TiO2-Ag nanoparticles. *Carbohydrate Polymers, 216*, 189-196.

Hosseini, S. F., & Gómez-Guillén, M. C. (2018). A state-of-the-art review on the elaboration of fish gelatin as bioactive packaging: Special emphasis on nanotechnology-based approaches. *Trends in Food Science & Technology, 79*, 125-135.

Huang, S., Xiong, Y., Zou, Y., Dong, Q., Ding, F., Liu, X., & Li, H. (2019). A novel colorimetric indicator based on agar incorporated with Arnebia euchroma root extracts for monitoring fish freshness. *Food Hydrocolloids, 90*, 198-205.

Jr, V. A. P., Arruda, I. N. Q. D., & Stefani, R. (2015). Active chitosan/PVA films with anthocyanins from Brassica oleraceae (Red Cabbage) as Time–Temperature Indicators for application in intelligent food packaging. *Food Hydrocolloids, 43*(1), 180-188.

Kanmani, P., & Rhim, J.-W. (2014). Properties and characterization of bionanocomposite films prepared with various biopolymers and ZnO nanoparticles. *Carbohydrate Polymers, 106*, 190-199.

Kubacka, A., Fernandez-Garcia, M., & Colon, G. (2011). Advanced nanoarchitectures for solar photocatalytic applications. *Chemical Reviews, 112*(3), 1555-1614.

Liu, J., Wang, H., Guo, M., Li, L., Chen, M., Jiang, S., Li, X., & Jiang, S. (2019). Extract from Lycium ruthenicum Murr. Incorporating κ-carrageenan colorimetric film with a wide pH–sensing range for food freshness monitoring. *Food Hydrocolloids, 94*, 1-10.

Liu, X., Chen, X., Ren, J., Chang, M., He, B., & Zhang, C. (2019). Effects of nano-ZnO and nano-SiO2 particles on properties of PVA/xylan composite films. *International Journal of Biological Macromolecules, 132*, 978-986.

Lizundia, E., Ruiznal of Biological Macromolecules, 132 C. (2019). Effects of nano-ZnO and nano-SiO2 particles on propertilding coatings for packaging applications. *Journal of Applied Polymer Science, 133*(2).

Lupan, O., Postica, V., Pauporté, T., Hoppe, M., & Adelung, R. (2019). UV nanophotodetectors: A case study of individual Au-modified ZnO nanowires. *Sensors and Actuators A: Physical, 296*, 400-408.

Oun, A. A., & Rhim, J.-W. (2017). Carrageenan-based hydrogels and films: Effect of ZnO and CuO nanoparticles on the physical, mechanical, and antimicrobial properties. *Food Hydrocolloids, 67*, 45-53.

Patel, A. K. (2015). Chitosan: Emergence as potent candidate for green adhesive market. *Biochemical Engineering Journal, 102*, 74-81.

Pourjavaher, S., Almasi, H., Meshkini, S., Pirsa, S., & Parandi, E. (2017). Development of a colorimetric pH indicator based on bacterial cellulose nanofibers and red cabbage (Brassica oleraceae) extract. *Carbohydrate Polymers, 156*, 193-201.

Quero, F., Padilla, C., Campos, V., Luengo, J., Caballero, L., Melo, F., Li, Q., Eichhorn, S. J., & Enrione, J. (2018). Stress transfer and matrix-cohesive fracture mechanism in microfibrillated cellulose-gelatin nanocomposite films. *Carbohydrate Polymers, 195*, 89-98.

Shankar, S., & Rhim, J.-W. (2017). Preparation and characterization of agar/lignin/silver nanoparticles

composite films with ultraviolet light barrier and antibacterial properties. *Food Hydrocolloids, 71*, 76-84.

Shankar, S., Teng, X., Li, G., & Rhim, J.-W. (2015). Preparation, characterization, and antimicrobial activity of gelatin/ZnO nanocomposite films. *Food Hydrocolloids, 45*, 264-271.

Tonon, R. V., Brabet, C., & Hubinger, M. D. (2010). Anthocyanin stability and antioxidant activity of spray-dried açai (Euterpe oleracea Mart.) juice produced with different carrier agents. *Food Research International, 43*(3), 907-914.

Valdez, M., Gupta, S. K., Lozano, K., & Mao, Y. (2019). ForceSpun polydiacetylene nanofibers as colorimetric sensor for food spoilage detection. *Sensors and Actuators B: Chemical, 297*, 126734.

Varma, R. S. (2012). Greener approach to nanomaterials and their sustainable applications. *Current Opinion in Chemical Engineering, 1*(2), 123-128.

Wang, H., Gong, X., Miao, Y., Guo, X., Liu, C., Fan, Y.-Y., Zhang, J., Niu, B., & Li, W. (2019). Preparation and characterization of multilayer films composed of chitosan, sodium alginate and carboxymethyl chitosan-ZnO nanoparticles. *Food Chemistry, 283*, 397-403.

Wei, Y.-C., Cheng, C.-H., Ho, Y.-C., Tsai, M.-L., & Mi, F.-L. (2017). Active gellan gum/purple sweet potato composite films capable of monitoring pH variations. *Food Hydrocolloids, 69*, 491-502.

Wu, S., Wang, W., Yan, K., Ding, F., Shi, X., Deng, H., & Du, Y. (2018). Electrochemical writing on edible polysaccharide films for intelligent food packaging. *Carbohydrate Polymers, 186*, 236-242.

Xiao-wei, H., Xiao-bo, Z., Ji-yong, S., Zhi-hua, L., & Jie-wen, Z. (2018). Colorimetric sensor arrays based on chemo-responsive dyes for food odor visualization. *Trends in Food Science & Technology, 81*, 90-107.

Yang, Z., Zou, X., Li, Z., Huang, X., Zhai, X., Zhang, W., Shi, J., & Tahir, H. E. (2019). Improved Postharvest Quality of Cold Stored Blueberry by Edible Coating Based on Composite Gum Arabic/Roselle Extract. *Food and Bioprocess Technology, 12*(9), 1537-1547.

Zeng, P., Chen, X., Qin, Y.-R., Zhang, Y.-H., Wang, X.-P., Wang, J.-Y., Ning, Z.-X., Ruan, Q.-J., & Zhang, Y.-S. (2019). Preparation and characterization of a novel colorimetric indicator film based on gelatin/polyvinyl alcohol incorporating mulberry anthocyanin extracts for monitoring fish freshness. *Food Research International, 126*, 108604.

Zhai, X., Li, Z., Shi, J., Huang, X., Sun, Z., Zhang, D., Zou, X., Sun, Y., Zhang, J., Holmes, M., Gong, Y., Povey, M., & Wang, S. (2019). A colorimetric hydrogen sulfide sensor based on gellan gum-silver nanoparticles bionanocomposite for monitoring of meat spoilage in intelligent packaging. *Food Chemistry, 290*, 135-143.

Zhai, X., Li, Z., Zhang, J., Shi, J., Zou, X., Huang, X., Zhang, D., Sun, Y., Yang, Z., Holmes, M., Gong, Y., & Povey, M. (2018). Natural Biomaterial-Based Edible and pH-Sensitive Films Combined with Electrochemical Writing for Intelligent Food Packaging. *Journal of Agricultural and Food Chemistry, 66*(48), 12836-12846.

Zhai, X., Shi, J., Zou, X., Wang, S., Jiang, C., Zhang, J., Huang, X., Zhang, W., & Holmes, M. (2017). Novel colorimetric films based on starch/polyvinyl alcohol incorporated with roselle anthocyanins for fish freshness monitoring. *Food Hydrocolloids, 69*, 308-317.

Zhang, J., Zou, X., Zhai, X., Huang, X., Jiang, C., & Holmes, M. (2019). Preparation of an intelligent pH film based on biodegradable polymers and roselle anthocyanins for monitoring pork freshness. *Food Chemistry, 272*, 306-312.

Zhang, X., Sun, G., Xiao, X., Liu, Y., & Zheng, X. (2016). Application of microbial TTIs as smart label for food quality: Response mechanism, application and research trends. *Trends in Food Science & Technology, 51*, 12-23.